Thermoluminescence and Apollo 17 ANGSA lunar samples: NASA's fifty-year experiment and prospecting for cold traps.

Derek W. G. Sears[1], Alexander Sehlke[1], Harrison H. Schmitt[2] and the ANGSA Science Team

[1]NASA Ames Research Center/ Bay Area Environmental Research Institute
Moffett Field, California 95035, USA.

[2]Department of Engineering Physics, University of Wisconsin-Madison, P.O. Box 90730, Albuquerque, NM 87199-0730, USA

Corresponding author: Derek W. G. Sears
Email: dsears@uark.edu

Version: 12th February 2024
Journal: *JGR – Planets (ANGSA Special Issue)*

Abstract

By placing Apollo 17 regolith samples in a freezer, and storing an equivalent set at room temperature, NASA effectively performed a fifty-year experiment in the kinetics of natural thermoluminescence (TL) of the lunar regolith. We have performed a detailed analysis of the TL characteristics of four regolith samples; a sunlit sample near the landing site (70180), a sample 3 m deep near the landing site (70001), a sample partially shaded by a boulder (72320), and a sample completely shaded by a boulder (76240).

We find evidence for a total of eight discrete TL peaks, five apparent in curves for samples in the natural state, seven in samples irradiated in the laboratory at room temperature. For each peak we suggest values for peak temperatures and the kinetic parameters E (activation energy, i.e. "trap depth", eV) and s (Arrhenius factor, s^{-1}). The lowest natural TL peak in the continuously shaded sample 76240 dropped in intensity by 60±10% (1976 vs. present room temperature samples) and 43±8% (freezer vs room temperature samples) over the 50-year storage period, while the other samples showed no change. These results are consistent with the E and s parameters we determined.

The large number of peaks, and the appearance of additional peaks after irradiation at room temperature, and literature data, suggest that glow curve peaks are present in lunar regolith at ~100 K and their intensity can be used to determine storage times at these temperatures. Thus a TL instrument on the Moon could be used to prospect for a micro-cold traps capable of deposition, build-up and storage of volatiles.

Plain Language Summary

Rocks, like the "soil" (regolith) from the Apollo 17 landing site, glow when heated in the dark. This glow, known as thermoluminescence (TL), is caused by previous exposure to radiation but it can fade depending on ambient temperatures. We therefore have a method for studying radiation and thermal history of these rocks, but we need to learn the precise details of this process. Nearly fifty years ago NASA placed some Apollo 17 regolith (1) in a metal cabinet at room temperature and (2) in a freezer. We found that freezer samples did not lose any TL, but the cabinet samples showed considerable fading relative to the freezer samples and relative to samples measured nearly fifty years ago. Combined with a detailed computer analysis of the data these results enable us to understand the relationships between TL, time, and environmental conditions. Most importantly, this method will enable us to search for tiny locations, called cold traps, in the polar regions of the Moon where water and other volatiles may have accumulated. This information is important for understanding the history of the Moon and it will support exploration efforts which need water and volatiles.

1. Introduction

Thermoluminescence (TL) is the light emitted by a sample as it is heated (Boyle, 1664; Herschel, 1899; Sears et al., 2013; also see the Supplement). A plot of light emitted vs. heating temperature is referred to as the "glow curve". Within the glow curve the luminescence is emitted as a series of peaks, each reflecting a different defect or impurity in the crystal structure where electrons can be "trapped". The level of luminescence naturally present in a given peak depends on previous exposure to radiation, which increases TL levels, or to heat, which decreases TL levels. Each peak has an activation energy E (eV, usually referred to as "trap depth") and an Arrhenius factor s (s^{-1}, essentially a rate constant) which describe the kinetics of light production. Thermoluminescence has practical applications in personnel dosimetry, pottery dating, and authenticity dating of artifacts (Aitken, 1985; Horowitz, 2021). When Apollo samples were returned from the Moon there was considerable interest in their TL properties (e.g., Hoyt et al., 1971; Durrani et al., 1972; Garlick and Robinson, 1972, Dalrymple and Doel, 1970; Blair et al., 1972a,b). Most publications dealt with TL as a means of investigating the thermal and radiation environment on and in the regolith (e.g., Hoyt et al., 1971; Durrani et al., 1976), while some considered TL as a possible explanation for transient lunar phenomena (Geake and

Mills, 1977; Geake et al., 1977). Batchelor et al. (1997) have used the induced TL (as opposed to natural TL) to deduce information on the petrologic and mineralogic history of lunar samples. Induced TL is the level of luminescence displayed by the sample after its natural TL had been removed by heating to 500 ^{o}C. Inducing a TL signal also reveals the existence of shallow electron traps that were empty in the natural sample.

This paper concerns regolith samples from the Apollo 17 landing site in the Taurus-Littrow valley (Schmitt, 1973; Wolfe et al., 1981). Harrison Schmitt and Gene Cernan collected $\geq$120 kg samples from the Taurus-Littrow valley in December 1972. In three EVAs they traversed about 30 km in order to sample ancient pre-and post-Imbrium highlands, basalts, and ejecta from the various impacts and pyroclastics deposits on the valley floor (Fig. S1). The present study concerns regolith (1) from the landing site, (2) from 3 m depth near the landing site, and from the foothills of (3) the North Massif and (4) the South Massif. The regolith consists of a mixture if subfloor basalt regolith, volcanic ash, regolith from of the nearby massifs and unconsolidated surficial material generated mainly from impact (Wolfe et al., 1981). The foothills sites were notable for the number of boulders that had rolled down the Massifs and some of our samples had been completely or partially, continuously shaded by the boulders for periods of about 20 Myr (North Massif) (Cozaz, et al., 1974) and 52 Myr (South Massif) (Leich, et al., 1975). Schmitt et al (2017) reported a synthesis of data related to the Apollo 17, 3 m deep drill core and found that it consists of 10 regolith ejecta zones laid down over about 3.3 billion years.

The most recent mass-wasting event originating from the slope of the South Massif is the “young” light mantle of avalanche-derived material, originally thought to have been deposited as a result of the impact of ejecta from Tycho Crater some ~2350 km to the southwest (Fig. S1; Arvidson et al., 1976; Drozd et al, 1977; Lucchitta, 1977). An ejecta ray from Tycho crosses Taurus-Littrow and some authors have argued that craters in the Crater Cluster, several kilometers east of the old and young light mantles, have similar ages to the Tycho impact. Alternatively, many large mass wasting events from the South Massif at different times may have deposited seven mass-wasting deposits,including the most recent, “young light mantle” investigated by Apollo 17 astronauts. The existence of the Lee-Lincoln thrust fault in the same part of the valley as these mass-wasting events suggests that repeated seismic activity along this fault may have triggered these events. Furthermore, recent work on the ages of 400-800 m diameter craters in the Crater Cluster and their regolith ejecta (sampled by the deep drill core), indicate that the Cluster is comprised of at least five different impact events, including four elliptical, apparently simultaneous impacts of that may be from a cometary aggregate. These new findings indicate that Tycho ejecta only could be responsible for only one of the mass-wasting events. Arguing against even that possibility is the youngest cosmice ray exposure age for ejecta from the Crater Cluster is 360 Myr (Eberhardt, et al., 1974) versus an age of ~52 Myr (Leich, et al., 1975) for the youngest mass-wasting event, the young light mantle.

Durrani et al. (1976) used TL measurements to discuss the thermal history of these samples pointing out that samples collected in the shadow of a large boulder had a stronger TL signal than partially shaded samples which in turn had slightly stronger signals than samples collected in direct sunlight. These authors described in some detail the theoretical underpinning of the measurements and how an equilibrium temperature (which they called "storage temperature") could be derived. Since the discovery of water on the Moon in permanently shadowed craters (Nozette et al., 1996; 2001), and the prediction of water-bearing micro-cold traps (Hayne et al., 2021), we have pointed out that TL could be used to prospect for locations suitable for the retention of water ice and other volatiles (Sehlke and Sears, 2022). Schmitt (2023) also stressed the value of thermoluminescence measurements in understanding the thermal history of the lunar regolith at high latitudes.

Durrani (1972) pointed out that it is possible that samples associated with particularly low temperatures or recent radiation exposure could have TL peaks that are unstable at room temperature and he therefore advocated storing returned lunar samples in a freezer. In the run-up to the return of humans to the Moon by Artemis, NASA made available samples of Apollo 17 regolith that had been stored in a freezer for nearly fifty years (1973-2022). They also released the equivalent room temperature samples. This provided a unique opportunity to characterize the natural TL of lunar samples and understand the kinetics of natural TL build-up and decay. This is essential if TL is to be used for science and exploration, particularly in the case of water and volatile prospecting.

2. Experimental

2.1. Samples

The samples used in this study are listed in Table 1 and their field relations are shown in Fig. S1 Three of these samples are equivalent to those used by Durrani et al (1976), sunlit (70180), partially shadowed (72321), and continuously shadowed (76240) regolith samples while the fourth is the sample from near the bottom of the 3 m drill core near the sunlit sample (70001). Available information on the samples have been compiled by Meyer (2007; 2010a; 2010b; 2010c; 2010d).

Table 1. Samples used in this study with some background information.

Room temperature	Mass (mg)	Freezer	Mass (mg)	Description*	CRE age† (Myr)	I_s/FeO‡
70001,83	100	70001,84	100	Deep regolith	~485	~40
70180,8	100	70180,9	106	Sunlit surface regolith	~360	47
72321,41	100	72320,7	108	Partially shaded surface regolith	45-55	73
76240,45	100	76240,48	112	Permanently shaded surface regolith	~20	56

* Meyer (2007; 2010a; 2010b; 2010c; 2010d)
† Arvidson et al. (1975), Leich et al. (1975); Crozaz et al. (1974).
‡ Morris (1976, 1978); Morris et al. (1979)

70001. This sample was the lowest level of the Apollo 17 three-meter drill core which was collected in the middle of the valley, near the landing site (Fig. S1). Much of the considerable early work on the drill core was summarized by McKay et al. (1991).

The Apollo 17 deep drill core was irradiated on 22 December 1972 using medical X-ray equipment facilities at JSC (Duke and Nagle, 1976). The dose absorbed was not reported, but a typical dose for the routine medical X-ray is about 1 Gy (Mettler et al., 2018), enough to fill the lower temperature traps, say those corresponding to peaks between 100-250 ºC in the glow curve. Since these peaks are absent or weak in 70001, we assume that in ~50 years these peaks have decayed.

Schmitt et al. (2017) estimate that this sample of the core is regolith ejecta that was exposed to external solar proton and cosmic ray radiation and impact gardening for ~387 Myr after deposition at ~3.4 Ga. In addition, there has been continuous internal alpha and beta particle radiation from U, Th and K decay. Prior to deposition, there also was an unknown frequency of periods of solar proton and cosmic ray radiation and impact gardening for the ~500 Myr since regolith began to form on the surface of the valley floor. After deposition, the sample was initially exposed to 387 Myr to a mean diurnal temperature of 214º K (~100º to ~375º K) (Langseth, et al., 1973) and then, at ~3.0 Ga, it began to be progressively buried by younger regolith ejecta zones until at about 1.5 Ga its temperature stabilized at a constant ~257º K (17º C) with more than 130 cm of regolith ejecta above it.

The mean-lives for these peaks we calculate below are consistent with this. Nevertheless, artificial exposure through the use of CT scanning must be kept in mind when discussing the radiation history of extraterrestrial samples from JSC and several major museums (see Sears et al., 2016; 2018).

70180. Regolith sample 70180 was collected on the surface near the drill core site (Fig. S1). Being a surface sample 70180 has suffered the full range of alteration, thermal cycling, micrometeorite bombardment, cosmic ray exposure, and gardening. In addition, solar protons and alpha radiation from internal sources (U, and Th) have caused reduction of Fe^{2+} to Fe^{o} (Schmitt, 2022) producing an Is/FeO maturity index of 56 (Morris, 1976).

72320 (and 72321). These samples were collected about 20 cm under the E-W overhang of Boulder 2 at Station 2 at the base of the South Massif (Fig. S1). On the basis of its intermediate natural TL compared to 70180 and 76240, Durrani et al. (1976) suggested that 72320 was only partially shaded, consistant with the astronauts' description during collection. The roughly N-S orientation of the overhang also indicates that morning sun would illuminate the otherwise largely shadowed area. The fully exposed top of the shadowing boulder has a cosmic ray exposure age of 52 ± 1.5 Myr (Leich, et al., 1975)

76240. This sample was from continuously shadowed soil from about 70 cm into a shadowed overhang under Boulder 4 at Station 6 at the foothills of the North Massif (Fig. S1). The sample came from the top 5 cm of the shadowed surface. Durrani et al. (1976) estimated that the shadow formed 40-60,000 years ago. However, as will be evident below, this value is a minimum age since the natural TL is in an equilibrium state. The maturity indexes of 76240 and other regolith samples at Station 6 strongly suggest that the shadow formed when the boulder came to rest and broke into several fragments between the boulder's reported cosmic ray exposure ages of ~20 Myr (Cozaz, et al., 1974).

2.2 – 2.4. Experimental details

Our methods for TL measurement are described in the supplement Sections S2.2 to S2.4. These include how we make a correction for black body radiation, how we fit theoretical curves to the observed glow curves, and how we estimate activation energies for the first peak in the glow curve using the traditional initial rise method.

3. Results

3.1. Visual Inspection of the glow curves

To provide ground truth for more sophisticated glow curve analysis we first performed a visual inspection of the glow curves to locate peaks and estimate their approximate relative intensities. Plots of the peak positions for natural and induced TL are shown in Fig. 1. Table S1 lists peak positions and peak intensities for natural TL. Table S2 lists the same data for induced TL.

As expected the natural TL for the room temperature and freezer samples are very similar. Average peak positions for samples in their natural state are 223±15, 270±18, 339±29, 413±14, 475±9 ºC. The glow curves for the irradiated samples show new peaks at 108±3, 147±2 and 192±2 ºC. We number these peaks 1-8 in order of increasing glow curve temperature.

The intensity of the TL in all our samples, natural and induced, is very high, ranging from about 1000 cps to about 50,000 cps. (For comparison the Dhajala meteorite, which is often used as a laboratory standard for TL studies, produces about 40,000 cps at its major peak.) For the natural TL samples the peak at 475±9 ^{o}C which extends beyond 500 ºC and is always the strongest while for the induced TL curves the three lowest temperature peaks are the strongest.

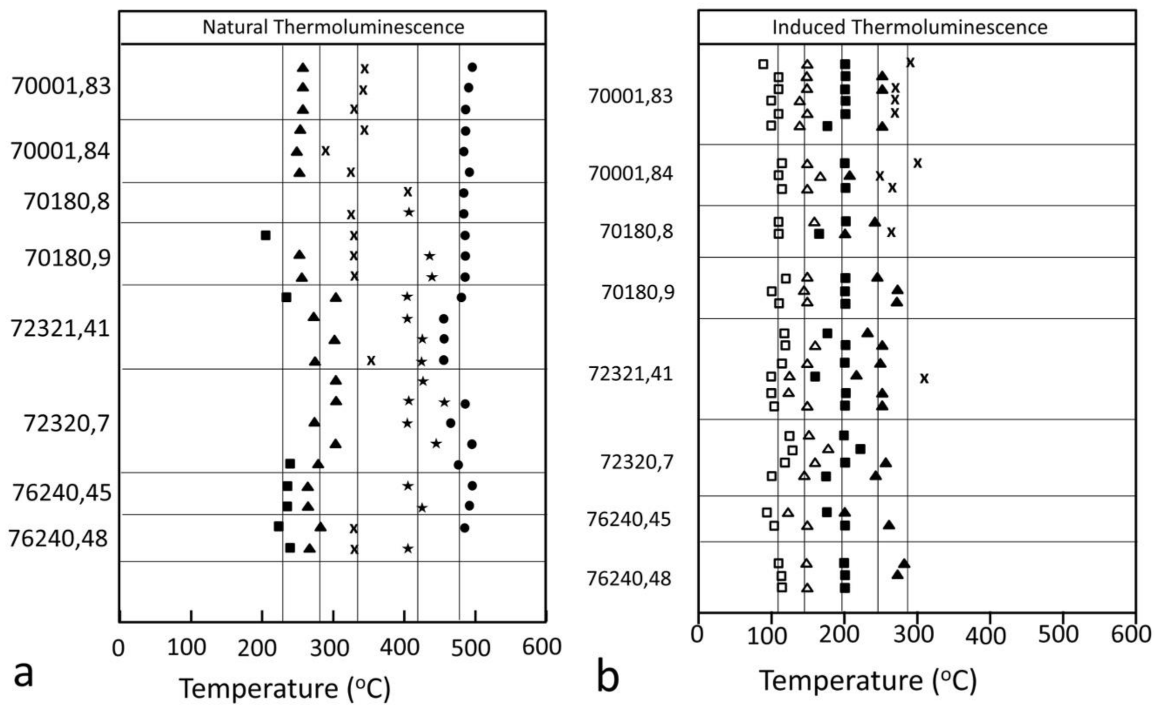

Fig. 1. (a) Visual representation of the peaks and inflections (indicative of peaks) for the present Apollo 17 samples. "Temperature" refers to the temperature at which the peak appears as the samples are heated. The vertical lines are means. Left, natural TL, mean ± 1 sigma, are 223±15, 270±18, 339±29, 413±14, 475±9 ºC. (b) TL peaks and inflections present after irradiating the samples with ^{90}Sr beta radiation, mean ± 1 sigma, are 108±3, 147±2, 192±2, 243±24, 289±43 ºC. As much as half of the 475±9 ºC peak actually lies beyond the range of our equipment.

3.2 Determination of E (and s) by the initial rise method

Estimates of the trapping depth E (in eV) of the first peak in the glow curve are given in Table 2. We also indicate in Table 2 the glow peak to which the data apply, i.e. the first significant peak identified by the curve fitting results. We also indicate s values calculated from E using Eqt. S4.

Table 2. Values of E (eV) determined by the initial rise method, corresponding s values, and peak temperatures, T_p.* †

Sample*		Room Temperature Samples	Freezer Samples	Irradiated samples Room Temperature & Freezer Samples
70001, 83/84	T_p	~220 ºC (peak 4)	~220 ºC (peak 4)	~100 ºC (Peak 1)
	E	0.98±0.20	1.18±0.08	0.95±0.06
	s	3×10^{9} ($2 \times 10^{7} – 4 \times 10^{11}$)	4×10^{11} (6×10^{10} - 2×10^{12})	4×10^{12} (6×10^{11} -2×10^{13})
70180,8/9	T_p	~420 ºC (Peak 7)	~420 ºC (Peak 7)	~100 ºC (Peak 1)
	E	1.03±0.01	1.05±0.31	0.86±0.11
	s	1×10^{10} (7×10^{9} - 1×10^{10})	2×10^{10} (8×10^{6} - 3×10^{13})	$2x 10^{11}$ (7×10^{9} - 9×10^{12})
72321,41/ 72320,7	T_p	~265 ºC (Peak 5)	~265 ºC (Peak 5)	~100 ºC (Peak 1)
	E	1.17±0.31	1.03±0.06	0.92±0.05
	s	3×10^{11} (2×10^{8} - 7×10^{14})	9×10^{9} (2×10^{9} - 4×10^{10})	1×10^{12} (3×10^{11} - 6×10^{12})
76240,45/48		~220 ºC (peak 4)	~220 ºC (peak 4)	~100 ºC (Peak 1)
	E	1.11±0.07	1.15±0.06	0.87±0.03
	s	7×10^{10} (1×10^{10} - 4×10^{11})	2×10^{11} (5×10^{10} - 7×10^{11})	3×10^{11} (2×10^{11} - 8×10^{11})
Mean ± sigma	E	1.08±0.07	1.10±0.06	0.90±0.02
Mean (*± 1s range*)	s	3×10^{10} (6×10^{9} - 1×10^{11})	6×10^{10} (1×10^{10} - 2×10^{11})	8×10^{11} (4×10^{11} - 1×10^{12})

* Tp refers to the peak to which these data apply as judged from Fig. 2.

† s has been calculated from E assuming peak temperatures of 225 ºC for natural curves and 100 ºC for induced curves and a heating rate of 7.5 ºC/s. The range in parenthesis refers to the values calculated for ±1s.

3.3. Curve fitting to natural TL curves

As discussed briefly in the Introduction, the TL of silicates is not emitted at a single heating temperature but over a broad range of temperatures and in the form of a number of overlapping peaks, each with its own value for E and s. The size of each peak, i.e. the number of electrons trapped at each defect, is governed by the kinetics of build-up due to ionizing radiations and thermal decay. Radiations are typically in the keV to GeV range and it is normally assumed that the ionization fills each trap according to their individual cross sections for electron capture. A relationship, proposed by Schmitt (2023), between trap filling and type and energy of radiation has yet to be experimentally explored.

Our procedure for fitting theoretical curves to the observed glow curve in order to identify and utilize the individual peaks is described in Section S2.4 and examples appear in Fig. 2. Our values for the activation energy, E, and rate constant, s, for the five peaks in the natural TL curves were the result of curve fitting to over 100 glow curves and are given in Table 3.

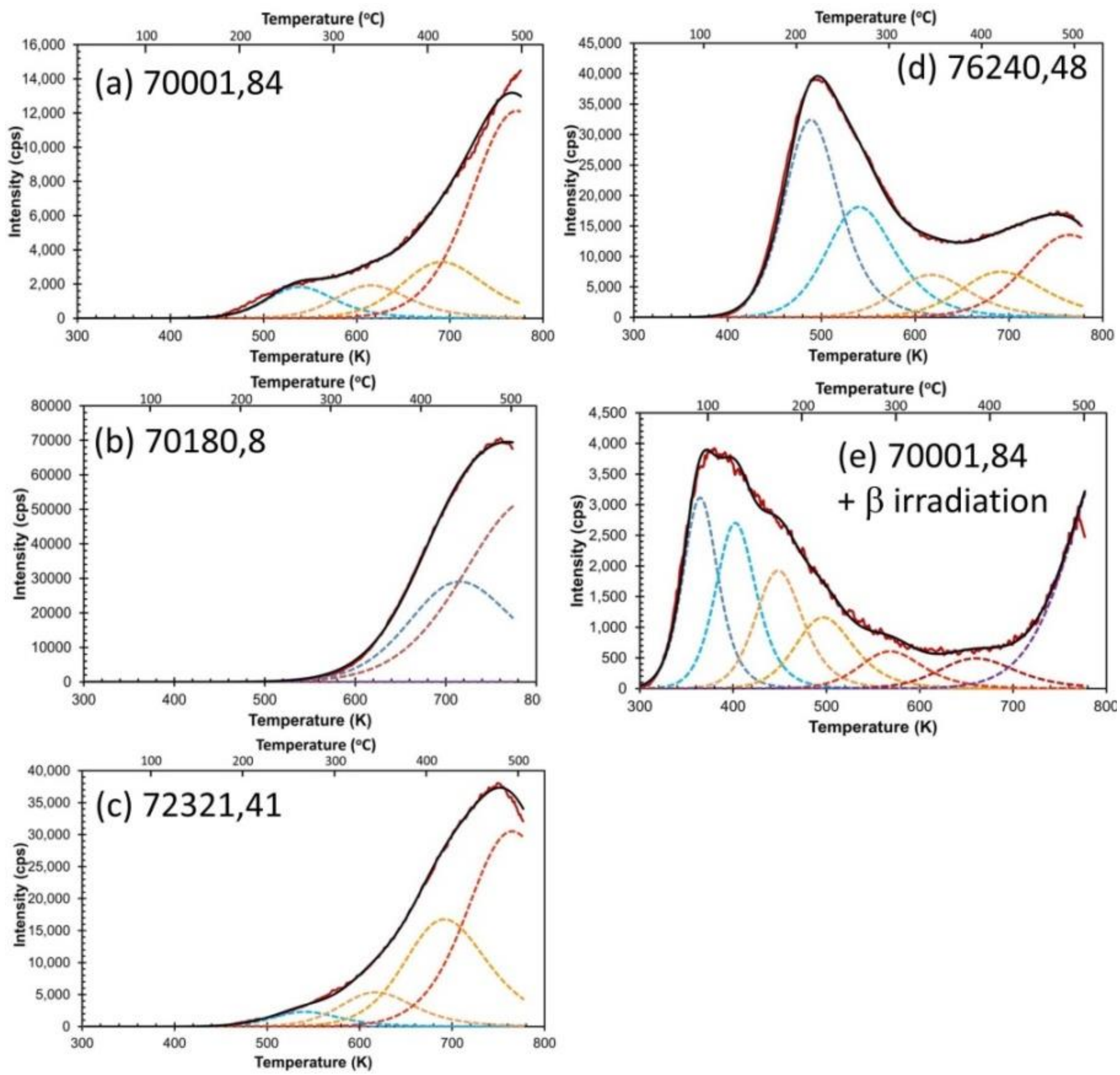

Fig. 2. Examples of curve fitting for samples in their natural states (Fig. a-d) and a sample that has been drained of its natural TL and given a test dose of beta radiation (Fig. e). The induced curves (Fig. e) look essentially the same for all samples. The individual peaks identified by the curve-fitting process are indicated with broken lines.

The curve fitting procedure does not yield uncertainties for the individual parameters but instead the software determines a measure for the quality of the fit between the theoretical and observed glow curve. For the natural glow curves all yielded a sigma of better than 0.5% which is consistent with the visual impression that the fits are excellent.

3.4. Curve fitting to induced TL curves

From curve fitting to over 300 glow curves our values for seven peaks in the induced TL curves are also given in Table 3. An example is shown in Fig. 2e. The fits obtained were not as good as for the natural curves but still acceptable with a 1σ goodness-of-fit of 1.0-1.5%. The main cause of the poorer fit was the higher temperature peaks which are sometimes weak or absent in the induced curves. Peaks 6 and 7 could not be resolved in the induced curves, although this was not a problem for the natural curves. In addition, the 500 ºC peak is only partially sampled since our equipment cuts-off at this temperature. This explains the discrepancy between the induced and natural E values for peak 8. Otherwise the values for natural and induced curves agree within experimental uncertainties. We note that s values differ by factors of 2 to 7 which we consider good agreement, since it is within an order of magnitude.

Table 3. Selected E, s and Tp values for natural and induced glow curves and corresponding mean lives.*

Natural TL					
Peak number	4	5	6	7	8
E (Ev)	0.95	0.94	1.13	1.26	1.39
s (s^{-1})	3.83×10^8	2.83×10^7	7.91×10^7	5.39×10^7	3.24×10^7
T_p (ºC)	216	268	344	419	492

Induced TL							
Peak number	1	2	3	4	5	6 and 7*	8†
E (Ev)	0.78	0.85	0.92	0.92	1.13	1.26	1.53
s (s^{-1})	9.95×10^9	5.13×10^9	1.85×10^9	1.41×10^8	5.83×10^8	1.61×10^8	6.11×10^7
T_p	92	130	175	223	295	387	498

* Comments

- Peaks 1 and 2 are absent in the natural curves. Peak 8 (at 492 ºC) is a composite of natural and induced TL since a single heating to 500 ºC removes only half the peak. Data for this peak should be treated with caution
- Peaks 5-8 in the induced curves are problematic because they are so weak. Peaks 6 and 7 are not resolved.
- For natural and induced curves the peak at 498 ºC is a composite of natural and induced TL since a single heating to 500 ºC removes only half the peak. Data for this peak should be treated with caution.

3.5 Total counts in the peaks by curve fitting.

Table S3 summarizes the n values (total number of counts, i.e., the area under each peak) we obtained from our curve fitting procedures, expressed in millions of counts. The number of counts in the natural curves varied from essentially zero to 7 million while the number for the induced curves varied from zero to about 3 million. In both cases the largest number of counts was observed for peak 8. In the natural curves peaks 1, 2 and 3 were always absent. The ratio of the sigma to the mean is about 0.28 for all peaks in the natural curves and about 0.25 for peaks 1-6 in the induced curves. For peak 7 in the induced curves this ratio is around 0.40 reflecting the known difficulties in measuring this peak.

4. Discussion

4.1. Comparison of the results of the visual inspection of the glow curve with the curve fitting results – validating the curve fitting technique

Having shown that the ~220 ºC peak is behaving as expected and the comparisons we have made using simple peak heights yields reasonable values for E and s for this peak, we now wish to perform a more detailed analysis of the glow curves with the aim of (1) understanding the TL characteristics of lunar regolith and (2) quantify the properties of the TL glow curve, that is the number of peaks, their E and s values, and the intensity of each peak. An important element of our approach is curve fitting. This has not previously been attempted with lunar samples and we expect regolith to be particularly challenging in view of its heterogeneous nature although the gardening process during exposure at the surface homogenizes most characteristic parameters, such as maturity index (Is/FeO), composition, and cosmic ray exposure. We will therefore establish some ground truth by comparing data obtained by visual inspection of the glow curve with data obtained by curve fitting. The main characteristics of the glow curve are peak positions (which also means number of peaks) and peak intensities.

Table 4. Comparison of peak positions (ºC) determined by eye and by curve fitting.*

	Peak 1	Peak 2	Peak 3	Peak 4	Peak 5	Peak 6	Peak 7	Peak 8
Visual natural				223±15	270±18	339±29	413±14	475±9
Curve fitting natural				216	268	344	419	492
Visual induced	108±3	147±2	192±2	230±12	271±5			
Curve fitting induced	92	130	175	223	295	387		498
Nominal value	~100	~140	~180	~220	~265	~340	~420	~480

* Uncertainties for the visual data are one sigma based on replicate measurements. Such uncertainties are not available for the peaks used in curve fitting (which are determined by the selected values for E and s) but the fits have an uncertainty of <5% so uncertainties on peak positions are probably on the order of 5%. Peaks 6 and 7 are not resolved in the induced curve fitting method because they are too weak.

Peak positions. The peak positions determined by eye (visual data) and by curve fitting are compared in Table 4. We can say that the data are consistent but not independent because peak positions determined by visual inspection guided the choice of peaks for curve fitting. Nevertheless, despite the uncertainties on the visual data sometimes bring quite large the consistency across methods is reassuring. These data are presented in visual form in Fig. S3. For future convenience, we also list “nominal” values in Table 4.

Peak intensities. Figure 3 is a plot of peak intensity measured directly from the glow curve against the number of counts in a peak determined by curve fitting. According to TL theory higher temperature peaks are broader than low temperature peaks but for each peak there is a linear correlation between the two parameters, suggesting no major errors in the curve fitting process.

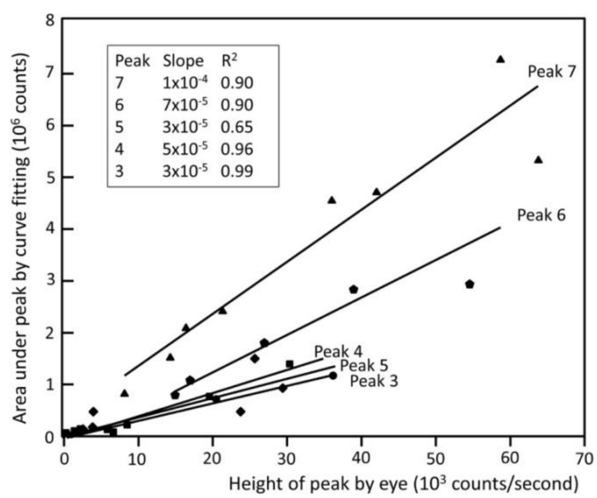

Fig. 3. Plot of number of counts in a peak (from curve fitting) against peak height (from visual inspection) for the five peaks in the TL glow curve. Each peak shows a positive correlation but, as expected from TL theory, the slope is steeper for higher temperature peaks. Peaks 1 and 2 and not shown for clarity but plot among the data for peaks 3-5.

4.2. Selected (preferred) values for E and s, and mean-lives

By comparing the results obtained with the natural samples, for the induced TL samples and the results obtained by the initial rise technique (see Table S5 for details) we suggest that (1) E values have 2σ uncertainties of ±5%; (2) s values are good to within a factor of two to three; (3) peak temperatures have 2σ uncertainties ±5 ºC. This is consistent with the data obtained by eye (Fig. 1). We summarize our selected values in Table 5. We are told that the storage facilities at

JSC have been kept at 293 K since 1969, although brief power outages from hurricanes may have caused some warming. We have also included the mean life, τ, of each TL peak for freezer temperature (253 K), room temperature (293 K), and lunar daytime equatorial temperatures (380 K which we have calculated from:

$$\tau = s^{-1} \exp(E / kT) \quad (1)$$

where k is Boltzmann's constant and T is the environmental temperature (in K). In the next two sections of our paper we consider whether our decay observations for peak 4 of the 76240 sample are consistent with our independent estimates of E and s.

Table 5. Selected values for E and s based on Table 2 and Table 3 and calculated mean lives calculated from Eqt (1)..

	Peak 1	**Peak 2**	**Peak 3**	**Peak 4**	**Peak 5**	**Peak 6**	**Peak 7**	**Peak 8**
E (eV)	0.85	0.85	0.92	1.1	1.2	1.1	1.2	1.4
s (s^{-1})	10^{11}	$5x10^{9}$	$2x10^{9}$	10^{9}	10^{10}	$8x10^{7}$	10^{8}	$3x10^{7}$
τ (253 K)	10 day	198 day	34 yr	259,490 yr	3 Myr	3 Myr	255 My	8,189 By
τ (293 K)	70 min	23 hour	39 day	265yr	1389 yr	3,308 yr	139,000 yr	1,276 Myr
τ (380 K)	2 sec	38 sec	13 min	51 day	10 day	56 day	3200 day	3900 yr

4.3. Comparison of glow curves from 1976 and now – the 46-year experiment

Comparing our data with the earlier data is not straight-forward because Durrani et al. (1976) reported light intensities in "arbitrary units" so absolute comparison is not possible. They also used different arbitrary units for each sample. We can side step this issue by comparing glow curve shapes rather than absolute values. This assumes that all glow curve peaks are caused by the same mineral in basalts but it is usually a safe assumption (Batchelor et al., 1997; Akridge et al., 2004), although minor contributions from silica (our unpublished observation) and apatite have occasionally be observed (Sears et al., 2021). Second, the earlier authors used a slower heating rate (3.6 ºC/s) than ours (7.5 ºC/s), however this is a minor effect that should not be significant for this first look at the data.

TL GLOW CURVE COMPARISON
Left column: 1976 vs now
Right column: 20 °C vs freezer

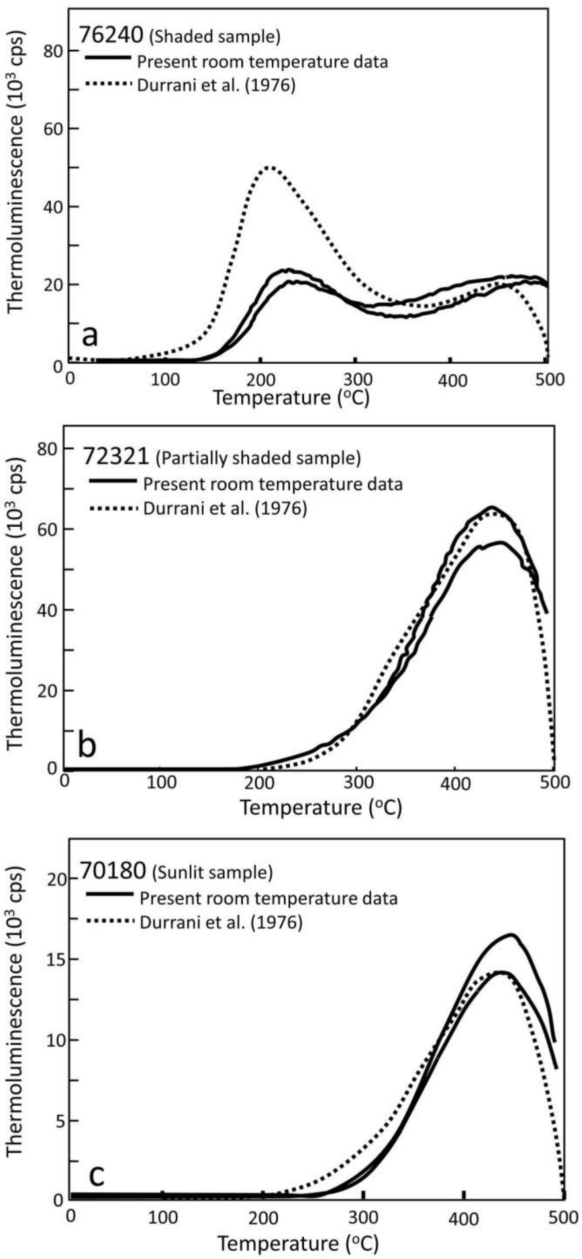

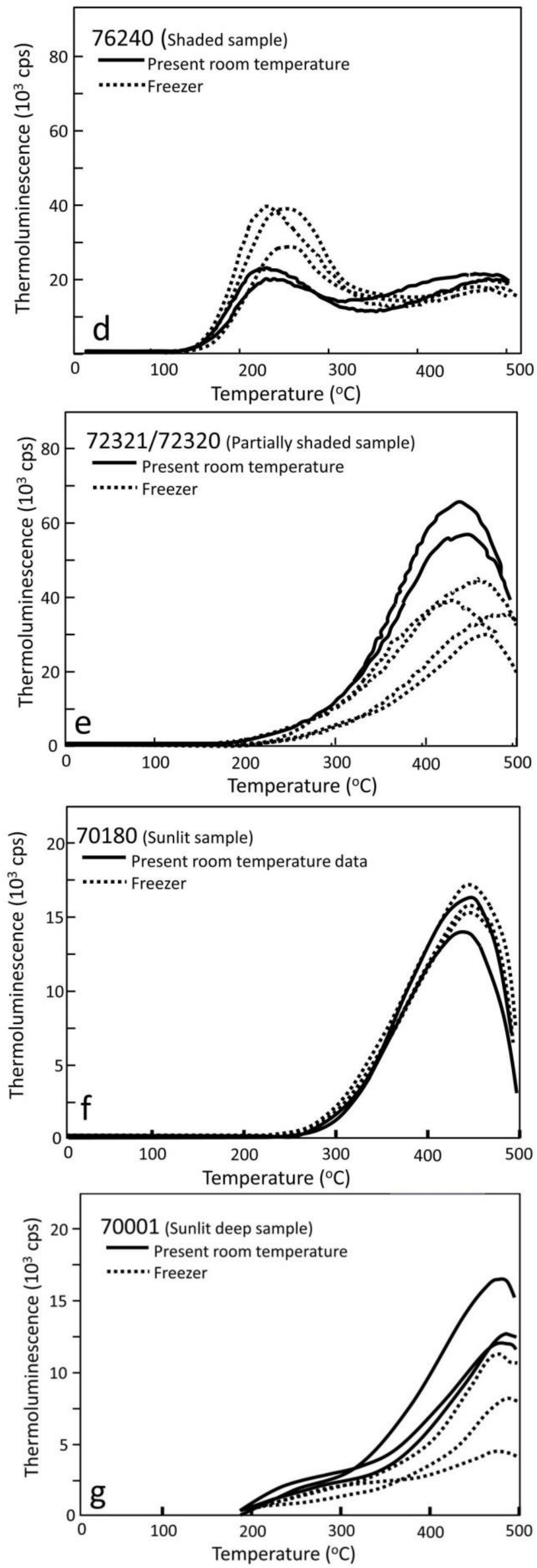

Fig.4. Left column: Comparison of glow curves for Apollo 17 samples collected in 1976 (Durrani et al., 1976) with data collected in 2022 for the samples stored at room temperature (20ºC). The left hand axis applies to the present data; previous authors used arbitrary units so here we compare curve shapes rather than intensities. The previous authors did not include 70001. Right column: Comparison of glow curves for Apollo 17 samples stored at room temperature with those stored in a freezer at -20ºC. Note c, f, and g have a different y-axis.

We compare the earlier data with the present glow curves in the left column of Fig. 4. We observe that the shaded sample (76240), with its strong peak in the ~220 ^{o}C region of the glow curve, appears to have faded by about 60% (Fig. 4a). We are comparing real data with a sketch, but if we assume the uncertainties on the sketch are comparable to ours, then the decay is 60±10%. This decay corresponds to a mean-life of about 55±9 years. Based on our present estimates for E and s, this peak (peak 4) has a mean-life of 50 years at 293 K. A ±5% error in E yields a range of 7 to 365 years, while an error of a factor of three in s yields a range of 17-168. In other words, considering the uncertainties in our data 50 years is in excellent (perhaps fortuitous) agreement with 60% decay.

We can actually use the observed decay measurements to calculate either E or s if we know the other. If we take our preferred value for E from Table 5 (1.10 eV) and substitute into Eqt, (1) we get s = 1.33 x 10^{9} s^{-1}, which is in excellent agreement with our preferred value of s in Table 5 of 10^{9} s^{-1}. Conversely, if we substitute our preferred value for s in Eqt. (1) we calculate a value of 1.01 eV which agrees within error of our preferred value. In other words, despite the rather large uncertainties on our independently determined values for E and s, they agree very well with the results of the fifty year experiment and the decay observed for the 220^{o}C TL peak of 76240.

The situation is very different for 72320/1 and 70180; Durrani et al. (1976) did not include 70001 in their study. The first peak for the sample from the partially shaded area (72320/1) is peak 5 (Table 2) with a mean life at room temperature (293 K) of 1389 years (Table 5). With a 5% error in E or a factor of three uncertainty in s the range is 192 to 10,000 years. The expected decrease in TL intensity over fifty years is 3.5% and it is unlikely we could have detected this given the sample heterogeneity. The first natural peak in the glow curve of the sunlit sample (70180) is peak 7 with a mean life at room temperature of 139,000 years. With a 5% error in E or a factor of three error in s, the range of uncertainty is 19,000 to 1.0 million years. Thus we expect to see no change in the natural TL of this sample over fifty years (the calculated value is (0.04%) and this is our observation

4.4. Compare room temperature and freezer samples:

The glow curves comparing the present room temperature samples with the sample kept in a freezer for almost fifty years are shown in the right side of Fig. 4 (i.e. Fig. 4d-g). Since all samples were measured on the same apparatus we do not need to normalize in any way.

There is scatter in the glow curves for some samples, this is especially true of the freezer samples for 72320 and 70001, and this can be explained by sample heterogeneity (as well as by vastly different lunar surface exposure histories) as can the differences between room temperature and freezer samples. Induced TL is a reflection of sample heterogeneity, not being affected by radiation and thermal history. As an example, the mean induced TL peak height for 70001 room temperature samples is 6100 counts while for the freezer samples it is 2200. By the same token, the induced TL of the three 70001 freezer samples are 2300, 2250, and 1800, which explains the scatter in these three glow curves. In summary, the scatter is easily explained by sample heterogeneity, given potential variability in mineral frequencies between the small sample sizes?. We conclude that 72320/72321, 70001 and 70180 show no significant difference in their glow curves. This is to be expected because of the long mean lives (Table 5). Using our preferred values for E and s, the mean life of peak 4 at freezer temperatures is 26,430 years. If we allow for a 5% uncertainty in E and a factor of 3 uncertainty in s, the range of possible mean lives is 2640 to 2.5 million years. The other peaks present in these samples have even longer mean lives (Table 5). Thus our E and s values are consistent with our observation that the peaks observed in natural TL curves for these samples are perfectly stable when the samples are stored in a freezer.

None of these arguments apply to the 220^{o}C peak of 76240 which reflects a true difference in thermal history for the *in situ*, freezer and room temperature samples. For 76240 the room temperature value is 43% lower than the freezer value (20.38±1.24 compared with 35.83±5.92, Table S1), or 43±8 % including uncertainties. This is similar to the value obtained for the then-and-now comparison of 60±10%, especially bearing mind that the old data is in the form of a sketch. The mean life for the freezer vs room temperature difference is 89±15 years. As described earlier, the room temperature mean life predicted by our independent determinations of

E and s is 50 years with a range of 7 to 365 years assuming an uncertainty in E of 5% and a factor of 3 for the uncertainty in s.

4.5. Estimating E or s directly from the decay observations?

NASA's fifty year experiment yields two results for the decay of peak 4 of the 76240 sample; the then-and-now experiment yields a mean life of 55±9 years and the freezer vs room temperature experiment yields a mean life of 89±15 years. These data do not alone enable us to determine the kinetics of this peak, but it does allow some check on our estimates of E and s by other means. Figure 5 plots Equation 1 for the mean-lives observed here. If we accept an s value of 10^8 s^{-1} (Table 5) and assume an uncertainty of a factor of three in either direction we find that E is 1.07±0.04 eV. This is in agreement with the independent laboratory determination of E using the initial rise method is which is 1.08±0.07 eV (room temperature samples) and 1.10±0.06 eV (the freezer samples) (Table 2).

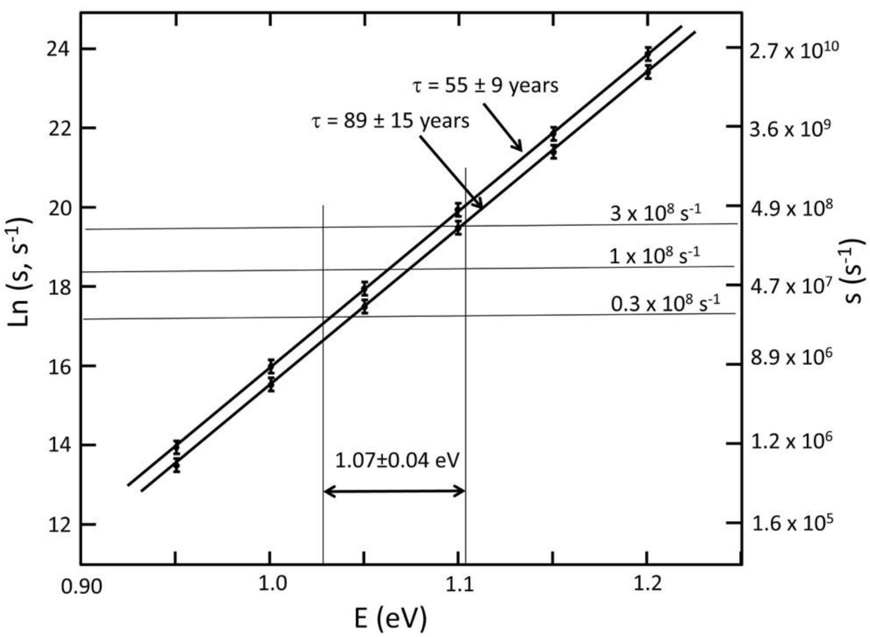

Fig. 5. Constraining E and s values using the mean-life observations reported here for the shaded sample 76240. Assuming s = 10^8 s^{-1} with an uncertainty of a factor of three (based on independent measurements), the trap depth of peak 4 is found to be 1.09±0.06 eV in agreement with the laboratory estimates using the initial rise method.

4.6. Induced TL and sample heterogeneity

A discussion of the induced thermoluminescence properties of these samples and the remainder of the Apollo 17 deep drill core appears in a companion paper (Sehlke and Sears, 2023). Essentially, the valley samples have induced TL similar to Maria samples while the samples from the foot hills of the massifs have highland values, a factor or five or so higher than the Mare samples. This is the case even given that the composition of the valley samples indicate significant mixing of the two types of regolith, ~30% Sculpured Hills regolith in valley sample 70180, for example. This difference can be attributed to different feldspar abundances. Some petrographic data for our samples is given in Table S4. These data are in agreement with the study of Batchelor et al. (1997). As one would expect of regolith samples there is a high degree of heterogeneity as evident from the uncertainties and the induced curves for the freezer samples 76240 (Fig. 4). This heterogeneity would be increased in the comparison of small samples.

4.7. Total peak intensities (total counts per peak).

Finally we compare the natural TL of samples stored at room temperature with the samples stored in a freezer using the n values (i.e. total counts in each peak) determined by curve fitting (Fig. 6). Error bars are not shown in the figure to avoid cluttering but are given in Table S3 (natural TL) and Table S4 (induced TL). We observe: (1) peak 4 in the 76240 sample (the peak that was of primary interest to Durrani et al. (1976) is lower for the room temperature data than for the freezer data by about 50%. This is in agreement with the peak shape observation described earlier (Fig. 4); (2) except for 76240, the room temperature and the freezer values for the natural TL are very similar; (3) as expected the induced TL data for the room temperature and freezer samples are very similar; (4) 76240 and 72320 have the natural and induced data which are higher by a factor of four or more than the Mare samples 70001 and 70180. This reflects the highland nature of 76240 and 72320 and with their relatively high abundance of feldspar; (5) We also know that there is very little overlap in the peaks present in the induced and natural TL data, just peak 4 and the scatter shown in the induced data for peak 4 is comparable with the analytical uncertainties, thus removal of the effects of heterogeneity by normalizing natural data to induced data is not possible.

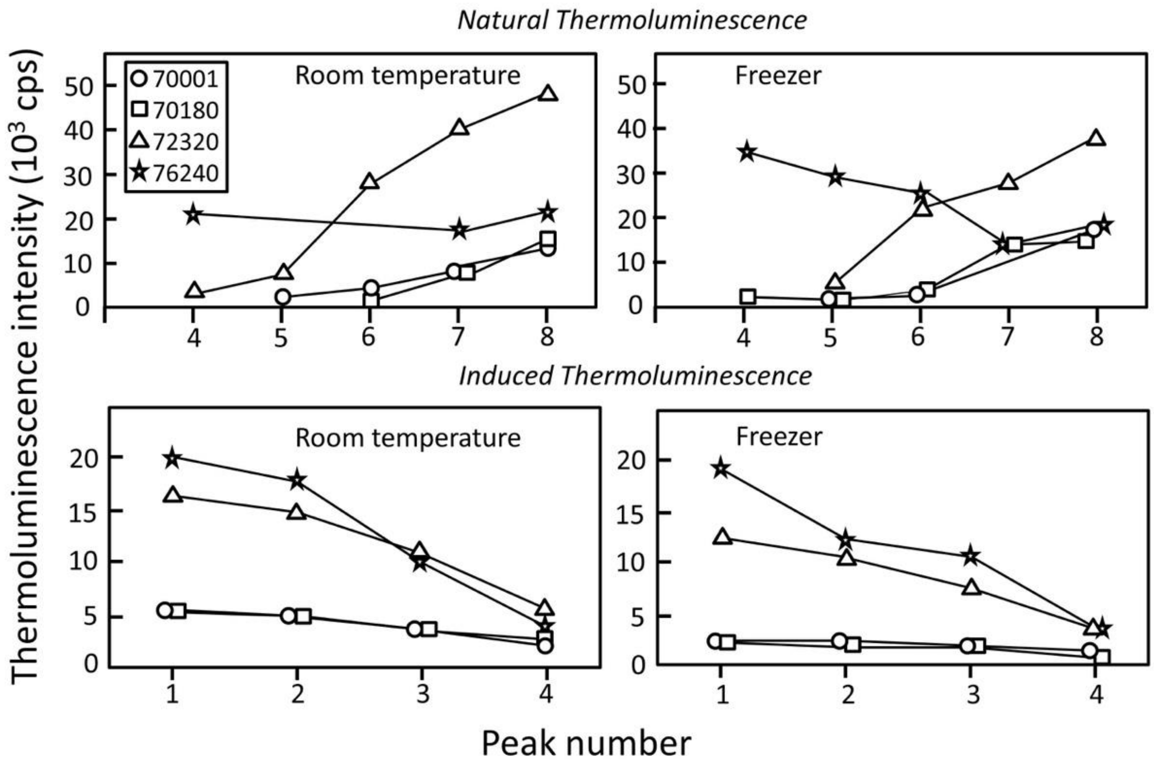

Fig. 6. Plots comparing the thermoluminescence intensity of the individual peaks (n values, areas under the peaks) determined by curve fitting. Peaks 1-3 are absent in the curves for samples in the natural state while peaks 5-8 are too weak to accurately measure for samples the which have had their natural signal removed and have been given a standard radiation dose in laboratory.

The reason for the difference between peaks 7 and 8 in the room temperature and freezer samples is unclear. The room temperature curves resemble the published sketch of the glow curve of 76240 by Durrani et al. (1976), given the thermal drainage of peak 4. However, we would expect peaks 7 and 8, which are thermally stable to be similar for the room temperature and freezer samples, especially given the similarity of the induced TL. Contamination by alien material is not a likely explanation for the difference, given the similarity of the induced curves. Instead, the contaminant material would have to have the same composition as the rest of the sample but a different (i.e. lower dose) radiation history. We are not clear how this could happen. We doubt very much that the radiationexposure in metal cabinets and the freezer the JSC laboratory was different. There are probably minor minerals such as quart and apatite (or whitlockite) present in the samples but our experience is that they have very different glow curve shapes.

These data demonstrate that while much of the behavior of lunar sample natural TL is understood, there remain anomalies that only further data and further work will resolve. This is not true of the presence or absence of individual peaks. We do not know what defect or impurity centers give rise to individual peaks, this is still a subject of active research field for solid state physicists interested in the ionic solids used in dosimetry. We are a long way from understanding these properties for silicate minerals and glass, although the spectroscopists have made a start (Geake et al., 1977). However, we now know that there are many TL peaks (eight between room temperature and 500 ºC) and we have a reasonable idea of their E and s values.

4.8. Equilibration temperatures at Taurus Littrow

Durrani et al. (1976) used the natural TL data for Apollo regolith to calculate storage temperatures (which we prefer to call equilibrium temperatures). The relevant relationship is:

$$T_{eq} = (E/k) / \{\ln [s R_{1/2} /0.693 r (N/n - 1)]\} \qquad (2)$$

Where E and s are the kinetic parameters, k is Boltzmann's constant, $R_{1/2}$ is the radiation dose required to half fill the traps, r is dose rate, and N/n is the reciprocal of the fraction of traps filled. We have eight TL peaks in the glow curves of the present samples starting at about 100 ºC. In principle, and as argued by Hoyt et al. (1971), the lower temperature TL peaks should be building up (i.e. growing faster than they are decaying), middle temperature peaks should be at equilibrium, and the highest temperature peaks should be "saturated", (i.e. decaying so slowly that they have reached a state where all the traps are filled). ***In general, the equilibration temperature of the lowest temperature peak <u>that is at equilibrium</u> will be the storage temperature for the whole sample.*** The challenge is to find a way of knowing which peaks are at equilibrium and which peaks are not. One approach is to make reasonable assumptions and test them by comparing T_{eq} with independent surface temperature estimates. Figure S6 summarizes some literature data in visual form.

On the surface of the Moon the external ? radiation dose rate as measured by Chang'E 4 at 45^{o} S 176^{o} E is 0.116 Gy/year (Zhang et al. 2020), close to the 1960s estimated global value of 0.10 Gy/year (Haffner, 1967). This value will be affected by latitude, surface composition, internal U+Th concentration, and local topography. The partial shielding effects of boulders will locally modify radiation dose rates at specific locations, for instance, but we expect dose rates to vary by less than an order of magnitude. For example. the TL profile across the 60 cm slab of the Estacado meteorite shows a variation of less than a factor of two (Sears, 1975).

Temperatures at the lunar surface range from -140 to 400 K (e.g. Bauch et al., 2014; see also Fig. S6). Near the poles, of course, temperatures are as low as 20-40 K are to be expected in the permanently shaded crater interiors. Of course, there are also burial depth effects, also summarized in Fig. S6. Soon after arrival on the Moon the Pragyan rover found that the temperature of the regolith at 69.37ºS,32.35ºE. dropped from 333 K to 263 K in only 10 cm (ISRO statement,2023). Temperatures stabalize, however, at about 257 K in the Apollo 17 hear flow probe (Langseth, et al, 1973).

Sunlit surface sample (70180,8). If we assume that peak 8 is at equilibrium then using our selected values for E and s given in Table 5, and allowing for an uncertainty of ±5% in E and a factor of 3 in s then T_{eq} is 370±10 K. This is in agreement with the TL estimate of 371 K by Durrani et al. (1976), and surface probes (384 K, Langseth et al., 1973; and 377 K (Song et al., 2017). The surface temperature obtained remotely for the center of the valley and reported by Bauch et al. (2014; see Fig S6a) is ~380 K. Peak 7 is also present in the glow curves of 70180 but it yields equilibration temperatures ~40 K lower suggesting that this peak is not at equilibrium. We note in passing that in a case where the heating follows a sine wave, it is the maximum temperature levels that dictate TL stability.

Buried sunlit surface sample (70001,83). A few meters below the surface the temperature of the lunar regolith remains constant. The models of Malla and Brown (2015) and Vasavado et al. (1999) indicate that while the surface cycles between ~100 K to ~380 K a few meters below the surface remains a constant ~250-257 K (Fig. S6b). Additionally there is a thermal gradient. Subsurface probes placed by the Apollo 17 astronauts indicated that while the surface was at ~240 K at the time of measurement, a few meters deep the recorded temperatures were ~270 K. (Keihm and Langseth, 1975; see Fig. S6c). The TL glow curve for this sample contains peaks 5 and 6, in addition to peak 8 (peak 7 could not be resolved), which have equilibration temperatures of 280 and 285 K respectively, both ±10 K, significantly higher than subsurface values measured with thermocouples. The difference might be that thermocouples yield real-time temperatures; TL is recording a time-averaged value (maybe ~10^4 years, see below). The low temperature edge of a ~650 cps plateau in the core (Sehlke A. and Sears, 1922) may reflect peak 4.

Partially shaded sample (72321,41). The equilibration temperature for peak 5, the first strong peak observed for this sample, is 280±10 K, well below the value for the sunlit sample from the middle of the valley and comparable with the 3 m deep sample. Durrani et al. (1976) did not report a temperature for this sample, but we assume it would be between 371 K (their sunlit sample) and 256 K (their shaded sample), although 256 is proably too high for the shaded sample as discussed above. In this sense, our value is as expected.

Fully shaded sample (76240,48). The first strong peak in this sample is peak 4 which yields an equilibration temperature of 266±10 K; the parameters for the trap indicate that at this temperature build-up due to radiation and decay due to thermal draining are in balance. Our value compares with the Durrani et al. (1976) estimate of 256±15 K. Thus the difference in temperature between the shaded and sunlit samples is on the order of 115 K. McGovern et al. (2013) used the Diviner radiometer on the Lunar Reconnaisance Orbiter to compare the temperatures of shadowed craters with adjacent planes Fig. S6d). These authors found a temperature difference of 75 to 120 K between the sunlit and shadowed areas. Again our TL data are consistent with other techniques.

4.9. Relationship between T_{eq} and log s and E

With current interest in water ice and the exploration of the lunar South Pole, we need to consider TL glow curves well below room temperature. Figure 7a looks more closely at the relationship between E, s and equilibration temperature. Very small values of s, say 10^4-10^6 produce equilibration temperatures that are strongly dependent on E being around 600 K for trap depths of 1 eV and 200 K for a very low trap depth of 0.3 eV. For the E and s values obtained here for peak 3, ~1 eV and ~10^8 s^{-1}, a temperature of ~500 K is indicated, in good agreement with Durrani et al. (1976). For much larger values for s, 10^{11} to 10^{13} say, the range of equilibration temperatures is smaller and varies from 100 to 325 K. How these E and s values relate to the peak temperatures is shown in Fig. 7b; this range of E and s values produced peak temperatures over the full range of ~100 K to 1000 K.

The bottom line of Fig. 7 is that with plausible values of E and s we can expect to see thermoluminescence peaks with equilibration temperatures as low as 100 K, a temperature at which water vapor would condense to ice assuming the regolith was at this temperature for sufficient time (Schorghofer and Taylor, 2007).

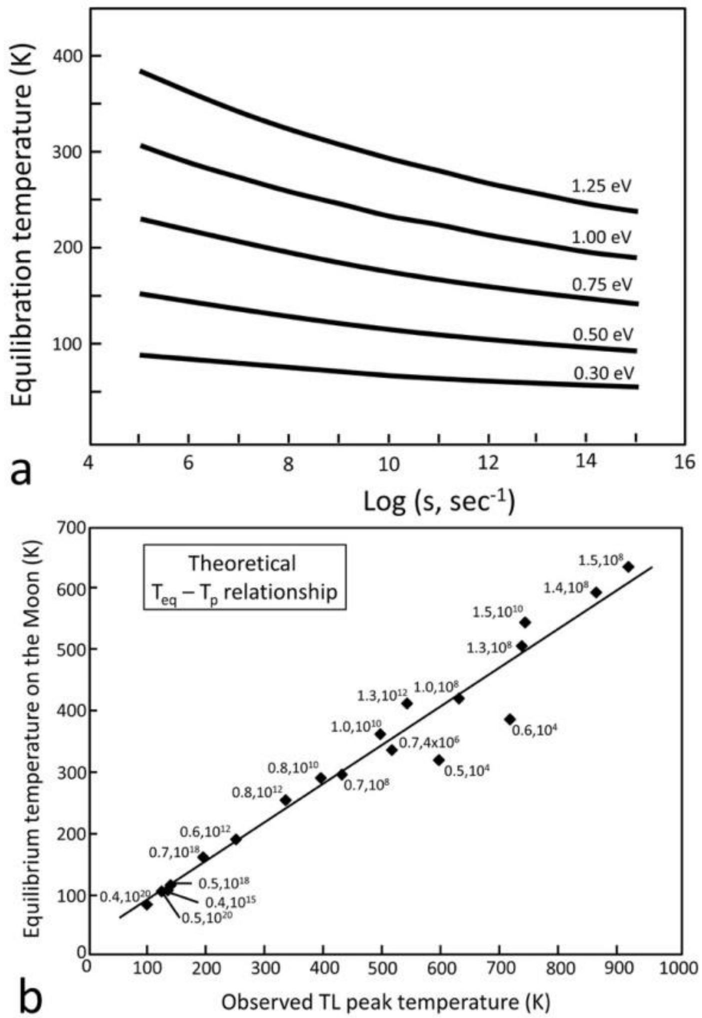

Fig.7. (a) The dependence of the equilibrium temperature for a natural TL peak on E and s. (b) Theoretical relationship between equilibrium temperature for natural TL peaks and peak temperature in the glow curve. Indicated by each data point are the assumed E (eV) and s (sec^{-1}) values.

4.10. Storage temperatures for returned lunar samples

Durrani (1972) and others recommended that NASA keep some of its lunar samples in a freezer and they agreed. This study is a result. Several of our samples were from the open lunar surface and had experienced temperatures of ~400 K and there was no advantage in freezing them. However, 76240 demonstrates that even rocks from the surface and at low latitudes (Apollo 17 landed at 20^o N, 31^o E), albeit in the shade, display a natural TL signal that decays at room temperature over 10s of years. Durrani's decay and mean-life arguments were based on samples he had artificially irradiated and known to have peaks that rapidly decay at room temperatures. He was, in effect, arguing that should sample ever be returned from colder regions they will need to be kept in a freezer on arrival on Earth or during transport there. Of course this becomes more critical if samples are returned from the lunar poles. In fact, even storage in liquid nitrogen might not be sufficient to retain an unaltered signal for samples from permanently shaded regions around the South Pole.

Since TL apparatus is robust, low power, low data rate and low weight, these temperature problems would be circumvented by instruments designed to be used on the lunar surface, either remotely or hand-held (Sehlke and Sears, 2022).

4.11. Time

The presence of water in the polar regions of the Moon depends not just of temperature but on time; the water vapor must have sufficient time to accumulate even when temperatures are favorable. Durrani et al. (1976) used the equation:

$$t = Ø / R \quad (3)$$

where t is time, Ø is dose (estimated from the natural TL using laboratory calibration), and R is the dose rate taken from Haffner (1967), which agrees closely with a recent lander measurement (Zhang et al., 2020). Durrani et al. (1976) obtained ages of 3.98×10^4 year for TL in the glow curve region 306-378 ^oC, which would be dominated by our peak 6, and 5.64×10^4 year for TL in the glow curve region 378-486 ^oC which encompasses our peaks 7 and 8. Peak 8 is subject to a number of difficulties because, like ours, their equipment cuts out at 500 ^oC. Durrani et al. (1976) assumed that these peaks were still growing when they considered these estimates as actual exposure ages; if the peaks were saturated (traps full) or at equilibrium (build-up equals decay) then they would be lower limits. Of course lower limits are also of value in determining the likelihood of water at a given cold trap.

In the supplement we calculate the non-equilibrium temperature at which mean-lives of the relevant peaks are comparable to the cosmic ray exposure ages. At the moment we have no scenario that would justify these comparisons but we hope this is the beginning of such a discussion, which should also include I_s/FeO values.

4.12. Prospecting for lunar cold traps

The normal lunar temperature range at the equator is 140 K to 400 K. Temperature in polar permanently shaded regions can be as low as 20-40 K (Sefton-Nash et al., 2019). Theoretical calculations suggest that water would be trapped under lunar conditions at ~100 K (Watson, et al., 1961; Arnold, 1971; Schorghofer and Taylor, 2007). From Fig. 7 we find that values of E in the order of 0.4 eV with a frequency factor of about 10^{20} would have an equilibrium temperature of ~100 K and correspond to a peak at 105 K in the TL glow curve.

Thus natural thermoluminescence with peaks in the vicinity of 100 K can serve as a thermometer. What is required is a quantitative understanding of peaks with E values of ~0.5 eV and s values in the order of 10^{18} to 10^{20} s^{-1}. However, knowing the temperature is not sufficient; we also need to know how long the regolith has been at that temperature. Natural TL also provides a means of determining time, as shown by Durrani et al. (1976). If the natural TL of a 100 K peak is known and using laboratory calibration is converted to dose, as is the practice in conventional use of TL as a dosimeter, then dividing by dose rate, which is well known as will be the internal concentration of U and Th, will give us the time during which the regolith was accumulation a TL signal. Durrani et al. (1976) found ages in the range 10^4-10^5 years for peaks the natural glow curves for Apollo 17 regolith samples; however, it is not clear that his technique can be applied to lunar TL data. Considerations of maturity indices and boulder dynamics indicate that the shadow for 76240 formed ~20 Myr ago. If the natural TL is at equilibrium then this time will be a lower limit, if the natural TL is still building-up, then the age will be a true age, although one must correct for decay during the buildup. Either way, it provides the answer to whether the regolith has been at these low temperatures long enough to accumulate volatiles.

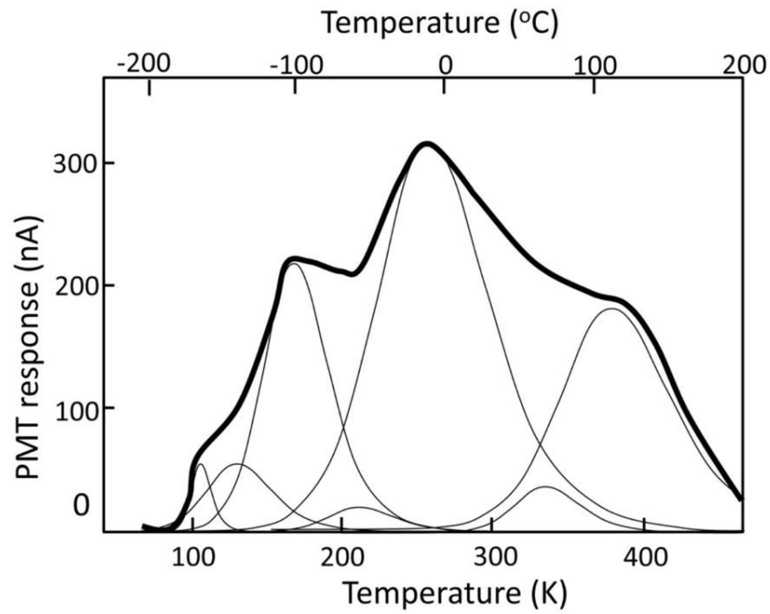

Fig. 8. Low-temperature TL glow curves for Apollo 15 regolith. Similar curves were obtained for Apollo 14 and 16 regolith samples. The heavy curve is the observed glow curve and the fine lines are our analysis in terms of individual peaks. (Blair et al., 1972a; sample A, 435-485 nm).

Thermoluminescence glow curve curves for Apollo 14, 15 and 16 regolith samples at liquid nitrogen temperatures have been published by Blair and his colleagues (Blair et al., 1972a,b). An example of their glow curves is shown in Fig. 8. These authors suggested that the curves could be resolved into four peaks but we suspect that several weaker peaks are also present. Clearly, TL down to 100K is displayed by these samples which would be suitable for cold trap prospecting. However, there are several caveats to be mentioned in comparing Blair's glow curves with ours. Their samples were irradiated to 0.75 krad with 160 MeV protons, the heating rate during measurement was 0.8 ºC/s and they mounted the samples for measurement with luminescent silicone grease. Thus detailed comparison is not justified, rather we show Fig. 7 to illustrate that low temperature measurements are possible and that TL in the 100 K region is present. We are also concerned that Blair et al. 1972b showed the same curve with a different temperature axis. Nevertheless with so many peaks in the room temperature to 500 ºC region of the glow curve there will be as many down to very low temperatures. Sun and Gonzales (1966) published a glow curve for the meteorite Cumberland Falls from -150 ºC to 250 ºC which showed many peaks below room temperature. While the luminescent phase was enstatite, not feldspar, this does indicate the feasibility of other silicate minerals having multiple peaks with very low equilibration temperatures.

5. Conclusions

We have conducted the first major study of the natural thermoluminescence of Apollo regolith samples using curve analysis as our major analytical technique. We have determined trap depths (i.e. activation energies) and pre-Arrhenius factors (i.e. rate constants) for the five TL peaks in natural samples and seven peaks in samples irradiated at room temperature with a laboratory radiation source. The results compare favorably with those obtained by traditional independent laboratory experiments.

The fifty-year experiment NASA organized for Apollo 17 samples, whereby some samples were stored at room temperature and others at -20ºC was successful. The sample of 76240 (the fully or continuously shaded sample) stored at room temperature showed an approximately 50% decay while the 76240 sample stored in the freezer show no measureable decay. This is consistent with the kinetic parameters we have derived and means that samples returned from shaded areas at any lunar latitude should be stored in a freezer if there is any possibility that studies of their radiation history will be performed in the future.

The relationships that have been developed during this work suggest that lunar cold traps could be located by astronaut-held or robotic thermoluminescence instrumentation. It seems that simple developments would enable this technique to be used in a remote fashion so that samples do not need to be handled.

6. Open Research

6. Open Research

6.1 Data Availability Statement: All experimental data, including glow curves and their metadata from this study, are publicly available at (Sehlke, 2024) under the CC BY 4.0 (Creative Commons Attribution 4.0 International) license.

6.2 Software Availability Statement: No software or models were used to generate the data discussed in this manuscript. The data analysis and interpretation methods employed are fully described in the Methods section of this manuscript for transparency and reproducibility.

Acknowledgements

We are pleased to have been involved in the ANGSA consortium with its leadership by Professor Charles "Chip" Shearer, and we appreciate the many meetings and workshops that have helped us think through the issues described here. We are also grateful to the several members of the community who have offered suggestions and encouragement, the JSC curatorial staff who have supplied samples sometimes under difficult circumstances, and the NASA program directors who worked patiently and carefully around COVID. This work was funded by the NASA Apollo Next Generation Sample Analysis (ANGSA) program.

References

Akridge, D.G., Akridge, J.M.C., Batchelor, J.D., Benoit, P.H., Brewer, J., DeHart, J.M., Keck, B.D., Jie, L., Meier, A., Penrose, M. and Schneider, D.M., 2004. Photomosaics of the cathodoluminescence of 60 sections of meteorites and lunar samples. *Journal of Geophysical Research: Planets*, *109*(E7).

Aitken, M.J., 1985. Thermoluminescence dating. Academic Press, Orlando, USA. 359 pp. number of pages.

Arnold, J.R., 1979. Ice in the lunar polar regions. *Journal of Geophysical Research: Solid Earth*, *84*(B10), pp.5659-5668.

Arvidson, R., Crozaz, G., Drozd, R.J., Hohenberg, C.M. and Morgan, C.J., 1975. Cosmic ray exposure ages of features and events at the Apollo landing sites. *The Moon*, *13*, pp.259-276.

Batchelor, J.D., Symes, S.J.K, Benoit, P.H., Sears, D.W.G., 1997. Thermoluminescence constraints on the thermal and mixing history of lunar surface materials and comparisons with basaltic meteorites. J. Geophys. Res. 102, 19,321-19,334.

Bauch, K.E., Hiesinger, H., Helbert, J., Robinson, M.S. and Scholten, F., 2014. Estimation of lunar surface temperatures and thermophysical properties: test of a thermal model in preparation of the MERTIS experiment onboard BepiColombo. *Planetary and Space Science*, *101*, pp.27-36.

Blair, I.M., Jahn R.A., Edgington, J.A. Durrani, S.A., Phillips N., and Kacperek A., 1972a. Thermoluminescence of Apollo 15 lunar samples:(I) -196 to 250 C. *The Apollo 15 Lunar Samples*, pp.453-456.

Blair, I.M., Edgington, J.A., Chen, R. and Jahn, R.A., 1972b. Thermoluminescence of Apollo 14 lunar samples following irradiation at-196 C. In Proceedings of the Lunar Science Conference, vol. 3, p. 2949 (Vol. 3, p. 2949).

Boyle R., 1664. Experiments and Considerations Touching Colours. Pub. Henry Herrington, London.

Crozaz G., Drozd R., Hohenberg C.M., Morgan C., Ralston C., Walker R.M. and Yuhas D. (1974) Lunar surface dynamics: Some general conclusions and new results from Apollo 16 and 17. *Proc. 5th Lunar Sci. Conf.* 2475-2500.

Dalrymple, G.B. and Doell, R.R., 1970. Thermoluminescence of lunar samples. *Science*, *167*(3918), pp.713-715.

Drozd, R.J., Hohenberg, C.M., Morgan, C.J., Podosek, F.A. and Wroge, M.L., 1977. Cosmic-ray exposure history at Taurus-Littrow. In *Lunar and Planetary Science Conference Proceedings* (Vol. 8, pp. 3027-3043).

Duke M.S. and Nagle J.S., 1976. Lunar core catalog, JSC 09252. NASA Johnson Soace Center, Houston, Texas.

Durrani, S.A., 1972. Refrigeration of lunar samples destined for thermoluminescence studies. *Nature*, *240*(5376), pp.96-97.

Durrani, S.A., Prachyabrued, W., Christo-Doulides, C., Fremlin, J.H., Edgington, J.A., Chen, R. and Blair, I.M., (1972). Thermoluminescence of Apollo 12 samples: implications for lunar temperature and radiation histories. In *Lunar and Planetary Science Conference Proceedings* (Vol. 3, p. 2955).

Durrani, S.A., Khazal, K.A.R. and Ali, A., (1976). Temperature and duration of some Apollo 17 boulder shadows. In *Lunar and Planetary Science Conference Proceedings* (Vol. 7, pp. 1157-1177).

Eberhardt, P., Eugster, O., Geiss, J., Graf, H., Grögler, N., Mörgeli, M. and Stettler, A., 1975, March. Kr81-Kr Exposure Ages of Some Apollo 14, Apollo 16 and Apollo 17 Rocks. In *Abstracts of the Lunar and Planetary Science Conference, volume 6, page 233,(1975)* (Vol. 6).

Garlick, G.F.J. and Robinson, I., 1972. The thermoluminescence of lunar samples. In *Symposium-International Astronomical Union* (Vol. 47, pp. 324-329). Cambridge University Press.

Geake, J.E. and Mills, A.A., 1977. Possible physical processes causing transient lunar events. *Physics of the Earth and Planetary Interiors*, *14*(3), pp.299-320.

Geake, J.E., Walker, G., Telfer, D.J. and Mills, A.A., 1977. The cause and significance of luminescence in lunar plagioclase. *Philosophical Transactions of the Royal Society of London. Series A, Mathematical and Physical Sciences*, *285*(1327), pp.403-408.

Haffner J.W., 1967. Radiation and Shielding in Space. Academic Press, New York.

Hayne, P.O., Aharonson, O. and Schörghofer, N., 2021. Micro cold traps on the Moon. *Nature Astronomy*, *5*(2), pp.169-175.

Heiken G.H. and McKay D.S. (1974) Petrology of Apollo 17 soils. *Proc. 5th Lunar Sci. Conf*. 843-860.

Herschel A.S., 1899. Triboluminescence. Nature 60, 29-29.

Horowitz, Y.S. ed., 2021. *Thermoluminescence and thermoluminescent dosimetry*. CRC Press.

Hoyt Jr, H.P., Miyajima, M., Walker, R.M., Zimmerman, D.W., Zimmerman, J., Britton, D. and Kardos, J.L., 1971. Radiation dose rates and thermal gradients in the lunar regolith: Thermoluminescence and DTA of Apollo 12 samples. In *Lunar and Planetary Science Conference Proceedings* (Vol. 2, p. 2245).

Keihm,S.J., Langseth,M.G.,1973. Surface brightness temperatures at the Apollo17 heat flow site: thermal conductivity of the upper 15 cm of regolith. in: Proceedings of the Lunar Science Conference. (GCA supplement 4), vol. 3, pp.2503–2513.

Keith J.E., Clark R.S. and Bennett L.J. (1974) Determination of natural and cosmic ray induced radionuclides in Apollo 17 lunar samples. *Proc. 5th Lunar Sci. Conf.* 2121-2138.

Langseth Jr, M.G., Keihm, S.J. and Chute Jr, J.L., 1973. Heat flow experiment. *NASA. Johnson Space Center Apollo 17 Prelim. Sci. Rept.*

Leich, D.A., Kahl, S.B., Kirschbaum, A.R., Niemeyer, S. and Phinney, D., 1975. Rare gas constraints on the history of Boulder 1, Station 2, Apollo 17. *The moon*, *14*, pp.407-444.

Lucchitta, B.K., 1977. Crater clusters and light mantle at the Apollo 17 site; a result of secondary impact from Tycho. *Icarus*, *30*(1), pp.80-96.

Malla, R.B. and Brown, K.M., 2015. Determination of temperature variation on lunar surface and subsurface for habitat analysis and design. *Acta Astronautica*, *107*, pp.196-207.

McGovern, J.A., Bussey, D.B., Greenhagen, B.T., Paige, D.A., Cahill, J.T. and Spudis, P.D., 2013. Mapping and characterization of non-polar permanent shadows on the lunar surface. *Icarus*, *223*(1), pp.566-581.

McKay D.S., Fruland R.M. and Heiken G.H. (1974) Grain size and the evolution of lunar soils. *Proc. 5th Lunar Sci. Conf.* 887-906.

McKay, D.S., Heiken, G., Basu, A., Blanford, G., Simon, S., Reedy, R., French, B.M. and Papike, J., 1991. The lunar regolith. *Lunar sourcebook*, *567*, pp.285-356.

Mettler Jr, F.A., Huda, W., Yoshizumi, T.T. and Mahesh, M., 2008. Effective doses in radiology and diagnostic nuclear medicine: a catalog. *Radiology*, *248*(1), pp.254-263.

Meyer, C (2007) Lunar Sample Compendium, 70001-70006 deep drill core (frozen samples) (https://curator.jsc.nasa.gov/lunar/lsc/ 70001-70006 deep drill core (frozen samples).pdf)

Meyer, C., 2010a. Lunar Sample Compendium, 70009 – 70001 Deep Drill Core 3 meters (https://curator.jsc.nasa.gov/lunar/lsc/70009.pdf)

Meyer, C., 2010b. Lunar sample Compendium. 70180 Reference Soil. https://curator.jsc.nasa.gov/lunar/lsc/70181.pdf

Meyer, C., 2010c. Lunar Sample Compendium, 72320 (https://curator.jsc.nasa.gov/lunar/lsc/72320.pdf)

Meyer, C., 2010d. Lunar Sample Compendium, 76240 (https://curator.jsc.nasa.gov/lunar/lsc/76240.pdf)

Morris R. V., 1976. Surface exposure indices of lunar soils: A comparative study. Ptoc. Lunar Sci. Conf. 7th, 315-335'

Morris R.V. (1978) In situ reworking (gardening) of the lunar surface: Evidence from the Apollo cores. Proc. 9th Lunar Planet. Sci. Conf. 1801-1811.

Morris R.V., Lauer H.V. and Gose W.A. (1979b) Characterization and depositional and evolutionary history of the Apollo 17 deep drill core. Proc. 10th Lunar Planet. Sci. Conf. 1141-1157.

Nozette, S., C. L. Lichtenberg, P. Spudis, R. Bonner, W. Ort, E. Malaret, M. Robinson, and E. M. Shoemaker (1996), The Clementine Bistatic Radar Experiment, Science, 274(5292), 1495–1498, doi:10.1126/science. 274.5292.1495.

Nozette, S., P. Spudis, M. Robinson, D. B. J. Bussey, C. Lichtenberg, and R. Bonner (2001), Integration of lunar polar remote-sensing data sets: Evidence for ice at the lunar south pole, J. Geophys. Res., 106(E10), 23,253–23,266, doi:10.1029/2000JE001417.

Schmitt, H.H., 2022. Taurus-Littrow data synthesis: Progress Report. *Apollo 17 ANGSA Workshop (2022), Abstract #2002.*

Schmitt, H.H., 2023. Continuously (" Permanently") Shadowed Lunar Regolith Sampled by Apollo 17: Key Tests of Regolith Temperature Storage for Artemis. *LPI Contributions, 2806*, p.2170.

Schmitt, H.H., Petro, N.E., Wells, R.A., Robinson, M.S., Weiss, B.P. and Mercer, C.M., 2017. Revisiting the field geology of Taurus–Littrow. *Icarus*, *298*, pp.2-33.

Schorghofer, N. and Taylor, G.J., 2007. Subsurface migration of H2O at lunar cold traps. *Journal of Geophysical Research: Planets, 112*(E2).

Sears, D.W. (1975) Thermoluminescence studies and the preatmospheric shape and mass of the Estacado meteorite. *Earth Planet Sci. Lett.*, **26**, 97-104.

Sears, D.W., Ninagawa, K. and Singhvi, A.K., 2013. Luminescence studies of extraterrestrial materials: Insights into their recent radiation and thermal histories and into their metamorphic history. *Geochemistry, 73*(1), pp.1-37.

Sears, D.W., Sears, H., Ebel, D.S., Wallace, S. and Friedrich, J.M., 2016. X- ray computed tomography imaging: A not- so- nondestructive technique. *Meteoritics & Planetary Science*, *51*(4), pp.833-838.

Sears, D.W., Sehlke, A., Friedrich, J.M., Rivers, M.L. and Ebel, D.S., 2018. X- ray computed tomography of extraterrestrial rocks eradicates their natural radiation record and the information it contains. *Meteoritics & Planetary Science*, *53*(12), pp.2624-2631.

Sears, D.W., Sehlke, A. and Hughes, S.S., 2021. Induced thermoluminescence as a method for dating recent volcanism: The Blue Dragon flow, Idaho, USA and the factors affecting induced thermoluminescence. *Planetary and Space Science*, *195*, p.105129.

Sefton-Nash, E., Williams, J.P., Greenhagen, B.T., Warren, T.J., Bandfield, J.L., Aye, K.M., Leader, F., Siegler, M.A., Hayne, P.O., Bowles, N. and Paige, D.A., 2019. Evidence for ultra-cold traps and surface water ice in the lunar south polar crater Amundsen. *Icarus*, *332*, pp.1-13.

Sehlke, A. (2024). Thermoluminescence and Apollo 17 ANGSA lunar samples: NASA's fifty-year experiment and prospecting for cold traps [Data set]. Zenodo. https://doi.org/10.5281/zenodo.10570313

Sehlke A. and Sears D. W. G., 2022. Thermal Histories of Lunar Cold Traps: Prospecting for Volatiles by Thermoluminescence. 54th Lunar and Planetary Science Conference, abs #5024.

Sehlke A. and Sears D. W. G., 2023. Lunar Regolith Thermoluminescence Glow Curve Fitting to Extract Its Most Important Kinetic Parameters 53rd Lunar and Planetary Science Conference, abs #1870

Song, Y., Wang, X., Bi, S., Wu, J. and Huang, S., 2017. Effects of solar radiation, terrestrial radiation and lunar interior heat flow on surface temperature at the nearside of the Moon: Based on numerical calculation and data analysis. *Advances in Space Research*, *60*(5), pp.938-947.

Sun, K.H. and Gonzalez, J.L., 1966. Thermoluminescence of the moon. *Nature*, *212*(5057), pp.23-25.

Vasavada, A.R., Paige, D.A. and Wood, S.E., 1999. Near-surface temperatures on Mercury and the Moon and the stability of polar ice deposits. *Icarus*, *141*(2), pp.179-193.

Watson, K., H. Brown and B. C. Murray (1961) The behavior of volatiles on the lunar surface, *Jour. Geophys. Res*., https://doi.org/10.1029/JZ066i009p03033

Wolfe E.W., Bailey N.G., Lucchitta B.K., Muehlberger W.R., Scott D.H., Sutton R.L and Wilshire H.G. (1981) The geologic investigation of the Taurus-Littrow Valley: Apollo 17 Landing Site. US Geol. Survey Prof. Paper, 1080, pp.280.

Zhang, S., Wimmer-Schweingruber, R.F., Yu, J., Wang, C., Fu, Q., Zou, Y., Sun, Y., Wang, C., Hou, D., Böttcher, S.I. and Burmeister, S., 2020. First measurements of the radiation dose on the lunar surface. *Science Advances*, *6*(39), p.eaaz1334.

ANGSA Science Team members. Names in bold indicate Project Science Group (PSG) members:

Name	**Email Address**	**Affiliation**
Alex Sehlke	sehlke@baeri.org	NASA Ames Research Center
Derek Sears	dsears@uark.edu	NASA Ames Research Center
Jessica Barnes	jjbarnes@lpl.arizona.edu	University of Arizona
Carolyn Crow	carolyn.crow@colorado.edu	University of Colorado Boulder
Maryjo Brounce	mbrounce@ucr.edu	University of California Riverside
Jeremy Boyce	jeremy.w.boyce@nasa.gov	NASA Johnson Space Center
Jed Mosenfelder	jmosenfe@umn.edu	University of Minnesota
Tom Zega	tzega@lpl.arizona.edu	University of Arizona
Zoë Wilbur	zewilbur@email.arizona.edu	University of Arizona
Sean Pomeroy	Sean.Pomeroy@colorado.edu	University of Colorado Boulder
Iunn Jenn Ong	oij4869@email.arizona.edu	University of Arizona
Timothy Hahn	timothy.m.hahn@nasa.gov	NASA Johnson Space Center
Timmons Erickson	Timmons.m.erickson@nasa.gov	NASA Johnson Space Center
Jamie Elsila Cook	jamie.e.cook@nasa.gov	NASA Goddard Space Flight Center
Daniel Glavin	Daniel.p.glavin@nasa.gov	NASA Goddard Space Flight Center
Jason Dworkin	Jason.p.dworkin@nasa.gov	NASA Goddard Space Flight Center

Jose Aponte	jose.c.aponte@nasa.gov	NASA Goddard Space Flight Center
Danielle Simkus	Danielle.n.simkus@nasa.gov	NASA Goddard Space Flight Center
Darby Dyar	mdyar@mtholyoke.edu	Mount Holyoke College/PSI
Antonio Lanzirotti	lanzirotti@uchicago.edu	University of Chicago
Stephen Sutton	sutton@cars.uchicago.edu	University of Chicago
Molly McCanta	mmccanta@utk.edu	University of Tennessee, Knoxville
Elizabeth Sklute	ecsklute@psi.edu	Planetary Science Institute
Kees Welten	kcwelten@berkeley.edu	University of California Berkeley
Kunihiko Nishizumi	kuni@berkeley.edu	University of California Berkeley
Marc Caffee	mcaffee@purdue.edu	Purdue University
Natalie Curran	natalie.m.curran@nasa.gov	Goddard Space Flight Center
Barbara Cohen	barbara.a.cohen@nasa.gov	Goddard Space Flight Center
Sarah Valencia	sarah.n.valencia@nasa.gov	University of Maryland
Catherine Corrigan	corriganc@si.edu	National Museum of Natural History
Emma Bullock	ebullock@carnegiescience.edu	Carnegie Earth and Planets Laboratory
Kate Burgess	kate.burgess@nrl.navy.mil	Naval Research Laboratory
Rhonda Stroud	stroud@nrl.navy.mil	Naval Research Laboratory
Brittany Cymes	brittany.cymes.ctr@nrl.navy.mil	Naval Research Laboratory
Jeffrey Gillis-Davis	j.gillis-davis@wustl.edu	Washington University St. Louis
Richard Walroth	rwalroth@stanford.edu	SLAC National Accelerator Laboratory
Thomas Kroll	tkroll@slac.stanford.edu	SLAC National Accelerator Laboratory
Dimosthenis Sokaras	dsokaras@slac.stanford.edu	SLAC National Accelerator Laboratory
Hope Ishii	ishii3@hawaii.edu	University of Hawaii
John Bradley	johnbrad@hawaii.edu	University of Hawaii
Roberto Colina-Ruiz	rcolina@stanford.edu	SLAC National Accelerator Laboratory
Charles Shearer	cshearer@unm.edu	University of New Mexico
Bradley Jolliff	bjolliff@wustl.edu	Washington University St. Louis
Mahesh Anand	mahesh.anand@open.ac.uk	Open University
James Carpenter	james.carpenter@esa.int	European Space Agency
Lars Borg	borg5@llnl.gov	Lawrence Livermore National Laboratory
Katherine Joy	Katherine.joy@manchester.ac.uk	University of Manchester
Lindsay Keller	lindsay.p.keller@nasa.gov	NASA Johnson Space Center
Paul Lucey	lucey@higp.hawaii.edu	University of Hawaii
Clive Neal	cneal@nd.edu	University of Notre Dame
Noah Petro	noah.e.petro@nasa.gov	NASA Goddard Space Flight Center
Harrison Schmitt	hhschmitt@earthlink.net	Harrison Schmitt Consulting
Richard Walker	rjwalker@umd.edu	University of Maryland
Alex Bradley	abradley@eps.wustl.edu	Washington University St. Louis
Adrian Brearley	brearley@unm.edu	University of New Mexico
William Cassata	cassata2@llnl.gov	Lawrence Livermore National Laboratory
Roy Cristofferson	roy.christoffersen-1@nasa.gov	NASA Johnson Space Center
Simon Clemett	simon.j.clemett@nasa.gov	NASA Johnson Space Center
Aidan Cowley	aidan.cowley@esa.int;	European Space Agency
Catherine Dukes	cdukes@virginia.edu	University of Virginia
Kate Freeman	khf4@psu.edu	Penn State University
Amy Gaffney	gaffney1@llnl.gov	Lawrence Livermore National Laboratory
Rhian Jones	rhian.jones-2@manchester.ac.uk	University of Manchester
Randy Korotev	korotev@wustl.edu	Washington University St. Louis
Thomas Kruijer	kruijer1@llnl.gov	Lawrence Livermore National Laboratory
Gordon Love	glove@ucr.edu	University of California Riverside
Dayl Martin	dayl.martin@esa.int	European Space Agency
Matthias Maurer	Matthias.Maurer@esa.int;	European Space Agency
Alex Meshik	ameshik@physics.wustl.edu	Washington University St. Louis
Alexandre Meurisse	Alexandre.Meurisse@esa.int	European Space Agency
Richard Morris	richard.v.morris@nasa.gov	NASA Johnson Space Center
James Papike	jpapike@unm.edu	University of New Mexico

Rita Parai	parai@wustl.edu	Washington University St. Louis
Olga Pravdivtseva	olga@wustl.edu	Washington University St. Louis
Zachary Sharp	zsharp@unm.edu	University of New Mexico
Justin Simon	justin.i.simon@nasa.gov	NASA Johnson Space Center
Steven Simon	bs8@unm.edu	University of New Mexico
Corliss Kin Sio	sio2@llnl.gov	Lawrence Livermore National Laboratory
Lingzhi Sun	lzsun@higp.hawaii.edu	University of Hawaii
Romain Tartèse	romain.tartese@manchester.ac.uk	University of Manchester
Kathie Thomas-Keprta	kathie.thomas-keprta-1@nasa.gov	NASA Johnson Space Center
Michelle Thompson	thomp655@purdue.edu	Purdue University
Kun Wang	wangkun@wustl.edu	Washington University St. Louis
Josh Wimpenny	wimpenny1@llnl.gov	Lawrence Livermore National Laboratory
Michael Cato	mcato@unm.edu	University of New Mexico
Anthony Gargano	agargano@unm.edu	University of New Mexico
Mason Neuman	mdneuman@wustl.edu	Washington University St. Louis
James McFadden	mcfadde8@purdue.edu	Purdue University
Dan Moriarty	daniel.p.moriarty@nasa.gov	NASA Goddard Space Flight Center
Giulia Magnarini	Giulia.magnarini.14@ucl.ac.uk	University College, London
Patrizia Will	Patrizia.will@wustl.edu	Washington University St. Louis
Zhen Tian	t.zhen@wustl.edu	Washington University St. Louis
Chris Yen	yence@wustl.edu	Washington University St. Louis
Abbey Flom	aflom@hawaii.edu	University of Hawaii
Chiara Ferrari-Wong	cfw@hawaii.edu	University of Hawaii
Jessika Valenciano	Jvalenc2@nd.edu	University of Notre Dame
Kamil Stelmach	kbs7dqw@virginia.edu	University of Virginia
Grace Minesinger	gmm9uf@virginia.edu	University of Virginia
Grant Killian	Gk3uk@virginia.edu	University of Virginia
Paul Carpenter	Paulc@levee.wustl.edu	Washington University St. Louis
Julian Rodriguez	smrodriguez@wustl.edu	Washington University St. Louis
Thomas Mitchell	tom.mitchell@ucl.ac.uk	University College, London
Peter Grindrod	p.grindrod@nhm.ac.uk	Natural History Museum London
Karen Ziegler	kziegler@unm.edu	University of New Mexico
James Dottin	jdottin@terpmail.umd.edu	Carnegie Earth & Planets Laboratory
Stu Webb	gwebb1@nd.edu	University of Notre Dame
Samantha Bell	samantha.bell@manchester.ac.uk	University of Manchester
Erick Cano	ejcano@unm.edu	University of New Mexico
Linda Ziamanesh	lsz9tp@virginia.edu	University of Virginia
Jessica Oraegbu	mfg9rv@virginia.edu	University of Virginia
Adam Woodson	akw8r@virginia.edu	University of Virginia
Jillian Maxson	jtm8hqg@virginia.edu	University of Virginia
Angelina Minocha	angelinam@wustl.edu	Washington University St. Louis
Ryan Ogliore	rogliore@wustl.edu	Washington University St. Louis
Caitlin Ahrens	Caitlin.ahrens@nasa.gov	NASA Goddard Space Flight Center
Francesca McDonald	Francesca.mcdonald@esa.int	European Space Agency
Advenit Makaya	Advenit.makaya@esa.int	European Space Agency
Nathan Bamsey	Nathan.bamsey@esa.int	European Space Agency
Thomas Rohr	Thomas.rohr@esa.int	European Space Agency
Gianluca Casarosa	Gianluca.casarosa@esa.int	European Space Agency
Matteo Appolloni	Matteo.appolloni@esa.int	European Space Agency
Robert Linder	Robert.lindner@esa.int	European Space Agency
Yuriy Butenko	Yuriy.butenko@esa.int	European Space Agency
Timon Schild	Timon.schild@esa.int	European Space Agency
Eoin Tuohy	Eoin.tuohy@esa.int	European Space Agency
Cyrille Crespi	Cyrille.crespi@esa.int	European Space Agency
Paul deMediros	Paul.demediros@esa.int	European Space Agency
Benoit Andre	Benoit.andre@esa.int	European Space Agency

Riccardo Biella	Riccardo.biella@esa.int	European Space Agency
Fiona Thiessen	Fiona.thiessen@esa.int	European Space Agency
Ryan Zeigler	ryan.a.zeigler@nasa.gov	NASA Johnson Space Center
Juliane Gross	juliane.gross@nasa.gov	NASA Johnson Space Center
Charis Krysher	charis.h.krysher@nasa.gov	NASA Johnson Space Center
Andrea Mosie	andrea.b.mosie@nasa.gov	NASA Johnson Space Center
Judith Allton	Judith.h.allton@nasa.gov	NASA Johnson Space Center
Scott Eckley	scott.a.eckley@nasa.gov	NASA Johnson Space Center
Jeremy Kent	jeremy.j.kent@nasa.gov	NASA Johnson Space Center
Julie Mitchell	julie.l.mitchell@nasa.gov	NASA Johnson Space Center
Cecilia Amick	cecilia.l.amick@nasa.gov	NASA Johnson Space Center
Ernest Lewis	ernest.k.lewis@nasa.gov	NASA Johnson Space Center
Romy Hanna	romy@jsg.utexas.edu	University of Texas, Austin
Richard Ketcham	ketcham@jsg.utexas.edu	University of Texas, Austin
David Edey	dave.edey@utexas.edu	University of Texas, Austin
Evan O'Neal	evan.w.o'neal@nasa.gov	NASA Johnson Space Center
Francis McCubbin	francis.m.mccubbin@nasa.gov	NASA Johnson Space Center
Tabb Prissel	tabb.c.prissel@nasa.gov	NASA Johnson Space Center